Computational inference of selection underlying the evolution of the novel coronavirus, SARS-CoV-2

Rachele Cagliani*[1#], Diego Forni*[1], Mario Clerici[2,3], Manuela Sironi[1]

[1] Scientific Institute IRCCS E. MEDEA, Bioinformatics, Bosisio Parini, Italy;

[2] Department of Physiopathology and Transplantation, University of Milan, Milan, Italy;

[3]Don C. Gnocchi Foundation ONLUS, IRCCS, Milan, Italy.

* These authors equally contributed to this work. Author order was determined alphabetically.

Address for correspondence: Rachele Cagliani (rachele.cagliani@lanostrafamiglia.it)

Running title: Molecular evolution of SARS-CoV-2

Abstract word count: 250

Text word count: 3151

Abstract

The novel coronavirus (SARS-CoV-2) recently emerged in China is thought to have a bat origin, as its closest known relative (BatCoV RaTG13) was described in horseshoe bats. We analyzed the selective events that accompanied the divergence of SARS-CoV-2 from BatCoV RaTG13. To this aim, we applied a population genetics-phylogenetics approach, which leverages within-population variation and divergence from an outgroup. Results indicated that most sites in the viral ORFs evolved under strong to moderate purifying selection. The most constrained sequences corresponded to some non-structural proteins (nsps) and to the M protein. Conversely, nsp1 and accessory ORFs, particularly ORF8, had a non-negligible proportion of codons evolving under very weak purifying selection or close to selective neutrality. Overall, limited evidence of positive selection was detected. The 6 *bona fide* positively selected sites were located in the N protein, in ORF8, and in nsp1. A signal of positive selection was also detected in the receptor-binding motif (RBM) of the spike protein but most likely resulted from a recombination event that involved the BatCoV RaTG13 sequence. In line with previous data, we suggest that the common ancestor of SARS-CoV-2 and BatCoV RaTG13 encoded/encodes an RBM similar to that observed in SARS-CoV-2 itself and in some pangolin viruses. It is presently unknown whether the common ancestor still exists and which animals it infects. Our data however indicate that divergence of SARS-CoV-2 from BatCoV RaTG13 was accompanied by limited episodes of positive selection, suggesting that the common ancestor of the two viruses was poised for human infection.

Importance

Coronaviruses are dangerous zoonotic pathogens: in the last two decades three coronaviruses have crossed the species barrier and caused human epidemics. One of these is the recently emerged SARS-CoV-2. We investigated how, since its divergence from a closely related bat virus, natural selection shaped the genome of SARS-CoV-2. We found that distinct coding regions in the SARS-CoV-2 genome evolve under different degrees of constraint and are consequently more or less prone to tolerate amino acid substitutions. In practical terms, the level of constraint provides indications about which proteins/protein regions are better suited as possible targets for the development of antivirals or vaccines. We also detected limited signals of positive selection in three viral ORFs. However, we warn that, in the absence of knowledge about the chain of events that determined the human spill-over, these signals should not be necessarily interpreted as evidence of an adaptation to our species.

Introduction

In December 2019, a human-infecting coronavirus, now referred to as SARS-CoV-2 (1), emerged in Wuhan, China, causing respiratory disease in a large number of people and being responsible for thousands of deaths (https://www.who.int/emergencies/diseases/novel-coronavirus-2019) (2). After SARS-CoV (severe acute respiratory syndrome coronavirus) and MERS-CoV (Middle East respiratory syndrome coronavirus), SARS-CoV-2 is the third coronavirus to cause a human epidemic in the last two decades (3, 4).

Coronaviruses (family *Coronaviridae*, order *Nidovirales*) have positive-sense, single stranded RNA genomes, which are unusually long and complex if compared to those of other RNA viruses. Two thirds of the coronavirus genome are occupied by two large overlapping open reading frames (ORF1a and ORF1b), that are translated into the pp1a and pp1ab polyproteins. These are processed to generate 16 non structural proteins (nsp1 to 16) (5). The remaining portion of the genome includes ORFs for the structural proteins: spike (S), envelope (E), membrane (M) and nucleoprotein (N), as well as a variable number of accessory proteins (3-5).

Several coronavirus genera and subgenera are recognized (https://talk.ictvonline.org/ictv-reports/) (1, 6, 7). Whereas MERS-CoV is a member of the *Merbecovirus* subgenus, phylogenetic analyses indicated that SARS-CoV-2 clusters with SARS-CoV and other bat-derived viruses in the *Sarbecovirus* subgenus (genus *Betacoronavirus*) (1, 8, 9). A recent report by the Coronavirus Study Group of the International Committee on Taxonomy of Viruses (ICTV) indicated that SARS-CoV-2 can be assigned to the species *Severe acute respiratory syndrome-related coronavirus* (1).

Bats host a large diversity of coronaviruses related to SARS-CoV (5, 10, 11) and, in general, these animals are believed to represent the original reservoir of several human-infecting coronaviruses (3, 4). This also seems to be the case for SARS-CoV-2, as analysis of the viral genome indicated that its known closest relative, with an average identity of ~96%, is a virus (BatCoV RaTG13) identified

in horseshoe bats (*Rhinolophus affinis*) (8). Two other bat-derived coronaviruses (bat-SL-CoVZC45 and bat-SL-CoVZXC21) display high levels of similarity (> 70%) to SARS-CoV-2, with identity varying along the genome (9, 12, 13). However, because both SARS-CoV and MERS-CoV were transmitted to humans via intermediate hosts (3, 4), it remains unclear whether the Wuhan epidemic was initiated by a spill-over from bats or from other animals. Recent data suggested that viruses related to SARS-CoV-2 are found in pangolins (*Manis javanica*), but the role of these animals in fueling the human epidemic remains unclear (14-17).

A major determinant of coronavirus host range is represented by the binding affinity between the spike protein and the cognate cellular receptor (18-22). Notably, this was previously shown to be the case for SARS-CoV, which, in analogy to SARS-CoV-2, uses ACE2 (angiotensin-converting enzyme 2) to enter host cells (8, 23). Few amino acid changes in the receptor binding domain (RBD) of SARS-CoV were shown to modulate the binding efficiency to ACE2 from different mammalian species and contributed to the adaptation of the virus to human cells (24-26). However, the SARS-CoV epidemic was characterized by another signature change in the viral genome: relatively early during the human-to-human transmission chain, SARS-CoV strains acquired a 29-nucleotide deletion which split ORF8, encoding an accessory protein, in two functional ORFs (27). Together with the observation that ORF8 is fast evolving in SARS-CoV strains, this finding was taken to imply adaptation to our species (28). The evidence for adaptation was subsequently questioned and recent data indicated that the 29-nucleotide deletion most likely represents a founder effect, which causes fitness loss irrespective of the host species (4, 29). These data underscore the relevance (and possible pitfalls) of evolutionary analyses in the study of viral species emergence and host shifts.

Herein, we used available SARS-CoV-2 strains to describe the selective events that accompanied the divergence of this novel human pathogen from its closets known relative (BatCoV RaTG13) (8).

Results and Discussion

As mentioned above, the closest relative (BatCoV RaTG13) of the novel human-infecting SARS-CoV-2 was identified in bats (8). It is presently unknown whether BatCoV RaTG13 can be transmitted in human populations and if it can infect human cells. Likewise, the reservoir and the animal host that fueled the human transmission of SARS-CoV-2 is presently uncertain. For sure, ample data now indicate that human-to-human transmission has a role in spreading the SARS-CoV-2 epidemic (30-33) and that, in addition to humans, the virus can infect cells from bats, small carnivores, and pigs (8). We thus set out to determine the selective events that accompanied the divergence of the SARS-CoV-2 lineage from BatCoV RaTG13. In doing so, we do not imply that any such event was primarily responsible for human adaptation, as high efficiency of human infection might instead represent an incidental byproduct of adaptation to another host.

Based on the alignment of forty-four SARS-CoV-2 genomes and the BatCoV RaTG13 sequence, 147 amino acid replacements, unevenly distributed along the genome, were found to separate SARS-CoV-2 from its closest relative. Forty-one amino acid changes are polymorphic in the SARS-CoV-2 population (Fig. 1A).

To investigate the selection patterns acting on SARS-CoV-2 genomes, we applied a method that combines analysis of within-population variation (i.e., variation among SARS-CoV-2 strains) and divergence from an outgroup (BatCoV RaTG13). Specifically, nucleotide alignments were analyzed using gammaMap (34), which estimates selection coefficients (γ) along coding regions and allows the detection of fine-scale differences in selective pressures at specific codons. In practical terms, γ values can be considered a measure of the fitness consequences of new nonsynonymous mutations. The method categorizes selection coefficients into 12 predefined classes ranging from -500 (inviable) to 100 (strongly beneficial). For gammaMap analysis, we divided the ORF1a and ORF1b alignments into the 16 nsps; because nsp3 is a long, multi-domain protein, it was also split into

domains. Likewise, the coronavirus S protein includes two functionally distinct units (S1 and S2), which were separately analyzed. Alignments of more than 80 codons were analyzed with gammaMap (Fig. 1A).

As previously shown for several other viruses (35-37), we found that most sites evolved under strong to moderate purifying selection ($\gamma < -5$). However, the strength of purifying selection varied depending on the region. The strongest constraints were observed for nsps 6 to 10, for nsp16, and for the M ORF (Fig. 1B). Whereas nsp6 is involved in the formation of the reticulovesicular membrane network where viral RNA replication occurs, nsp7 to nsp10 are small proteins that function as cofactors for viral replicative enzymes, including nsp16, a 2′-O-methyl transferase (38). Conversely, the M ORF encodes a structural protein, which is highly abundant in the in the virion of coronaviruses (39). The M protein interacts with other structural viral proteins and plays an important role in virion morphogenesis (40). Importantly, the M protein is a dominant immunogen for both the humoral and the cellular immune responses (41, 42). These latter features and its high level of constraint suggest that the M protein represents an excellent target for vaccine design.

Among the non-accessory ORFs, the lowest levels of constraint were observed for nsp1 and the acidic domain of nsp3 (Fig. 1B and 1C). This is in line with evidences indicating that these regions are fast evolving in coronaviruses at large (see below) (43, 44). Accessory ORFs, and in particular ORF8, had a non-negligible proportion of codons evolving under very weak purifying selection or close to selective neutrality. On one hand, this is in line with the idea that genetic variation in accessory ORFs causes limited fitness consequences, as the above-mentioned case of SARS-CoV ORF8 indicates (4, 29). In fact, gains and losses of accessory proteins have been common during the evolutionary history of coronaviruses and accessory ORFs differ in number and sequence even among coronaviruses belonging to the same genus or subgenus (4). On the other hand, accessory proteins were often shown to contribute to the modulation of immune responses, as well as to virulence (3, 4). It is thus conceivable that their limited constraint maintains variability in

coronavirus accessory ORFs, eventually facilitating rapid adaptation when the environment (e.g., host) changes.

We next wished to determine whether positive selection at specific sites also drove the evolution of SARS-CoV-2. We thus estimated codon-wise posterior probabilities for each selection coefficient. Very strong evidence (defined as a posterior probability > 0.80 of $\gamma \geq 1$) of positive selection was detected for seven sites, six in the S1 region of the spike protein and one in N (Fig. 2). When the posterior probability cutoff was lowered to a less stringent value of 0.50, five additional sites in ORF8 (4) and in nsp1 (1) were identified (Fig. 2). It should be noted that this p value cutoff represents a reasonably strong evidence of positive selection. Using these criteria, positively selected sites were estimated to account for the 0.12% of analyzed codons if 0.5 is used as the cutoff (0.07% for a 0.8 cutoff) (34, 45, 46).

The S1 region contains the RBD, and crystal structure of the SARS-CoV S protein in complex with human ACE2 showed that, in turn, the RBD is formed by two subdomains, a core structure and the receptor-binding motif (RBM, that directly contacts ACE2) (47, 48). The S2 region includes the fusion machinery (49). We performed homology modeling of the SARS-CoV-2 S protein onto the SARS-CoV structure and we analyzed the distribution of selection coefficients (Fig. 3A). The S2 subunit was characterized by stronger constraint than the S1 portion and five out of six putative positively selected sites were found to be located in the RBM, at the binding interface with ACE2 (Fig. 3A).

When SARS-CoV-2 and BatCoV RaTG13 are compared, the RBM stands out as the single most divergent region (Fig. 1A)(8, 16). Very recent evidence indicated that, although the average genome similarity is lower compared to BatCoV RaTG13, coronaviruses isolated from pangolins have RBMs almost identical to that of SARS-CoV (14-17). This clearly implies that recombination might have inflated the estimation of positive selection in the S1 region. A pangolin virus available in GenBank (isolate MP789) has an RBM with high identity to SARS-CoV-2. Thus, using the genome

sequence of isolate MP789, SARS-CoV-2 and BatCoV RaTG13 we searched for recombination events using RDP4 (50). No evidence of recombination was detected, but this finding might be due to the fact that the parental sequence with which BatCoV RaTG13 recombined is presently unsampled. We thus analyzed synonymous substitutions in the RBM alignment for these viruses: we found that 41% (n= 37) of such substitutions are shared between SARS-CoV-2 and isolate MP789, whereas only 27% (n= 10) are shared between SARS-CoV-2 and BatCoV RaTG13. Overall, these findings strongly suggest that recombination rather than positive selection shaped the genetic diversity at the RBM, as previously suggested (16). Recombination is known to affect evolutionary inference (51). In this case, because we used the BatCoV RaTG13 as an outgroup, the spurious signals were generated by considering the selected sites as amino acid replacements that arose and fixed in the SARS-CoV-2 population, whereas they may represent changes that occurred in the outgroup through recombination. We consider that this is not the case for the other signals we detected, as all of them were located in regions of high overall similarity between BatCoV RaTG13 and SARS-CoV-2, indicating no evidence of recombination (Fig. 1A).

The positively selected site (A267) in the nucleocapsid protein is located in the C-terminal domain. Homology modeling using the SARS-CoV N protein as a template indicated that A267 is located on an exposed loop on the protein surface (Fig. 3B)(52). The N protein is the most abundant protein in coronavirus-infected cells (53, 54). Its primary function is to package the viral genome into a ribonucleoprotein complex. In addition, the N protein performs non-structural functions, as it regulates the host cell cycle and the stress response, it acts as a molecular chaperone, and it interferes with the host immune response (53, 54). Because these activities are mediated by interaction with different cellular proteins, the positively selected site might be evolving to establish, maintain, or avoid the binding of different host molecules.

Another positively selected site was detected in the nsp1 region, which also displayed relatively weak selective constraint. In SARS-CoV and other betacoronaviruses, nsp1 is a virulence factor and

is essential for viral replication at least in the presence of an intact host interferon (IFN) response (55-57). Despite their relevant role for viral fitness *in vivo*, nsp1 proteins tend to be variable in sequence both within and among coronavirus genera. Detailed analysis of SARS-CoV nsp1 indicated that the protein plays multiple roles during viral infection, including inhibition of host protein synthesis, antagonism of IFN responses, modulation of the calcineurin/NFAT pathway, and induction of chemokine secretion (43). Homology modeling using the SARS-CoV nsp1 structure indicated that the positively selected site (E93) is exposed on the protein surface (Fig. 3C). Extensive mutagenesis of SARS-CoV nsp1 showed that exposed charged residues, including the positively selected site, mediate inhibition of gene expression and antiviral signaling (58). Moreover, the N-terminal half of SARS-CoV nsp1 interacts with immunophilins and calcipressins to modulate the calcineurin/NFAT pathway (59). Overall, these observation suggest that the diversity of coronavirus nsp1 proteins is driven by the need to establish interactions with multiple cellular partners and to evade immune surveillance. This is also likely to explain the positive selection signal we detected. In general, a better understanding of the evolutionary constraints and forces acting on coronavirus nsp1 proteins may be extremely relevant, as the generation of viruses carrying nsp1 mutations was regarded as a potential strategy to generate attenuated vaccine strains (57, 60), and inhibitors of cyclophilins were considered as potential antivirals for coronavirus treatment (59).

Finally, the selected sites we identified in ORF8 (F3, I10, A14, T26) are all located in the N-terminal portion of the protein (Fig. 2). The SARS-CoV-2 ORF8 protein displays 30% identity to the intact ORF8 from the SARS-CoV GZ02 stain. It is presently unsure whether the SARS-CoV ORF8 N-terminus is cleaved as a signal peptide or inserted in the endoplasmic reticulum membrane (61, 62). Using computational methods to predict signal peptides and transmembrane helices we found evidence for both in the case of the N-terminus of SARS-CoV-2 ORF8 (not shown). Clearly,

experimental analyses will be required to determine the function of the N-terminal region of ORF8, and, more generally the relevance of the selected sites on virus fitness or pathogenicity.

Overall, our analyses indicate that distinct coding regions in the SARS-CoV-2 genome evolve under different degrees of constraint and are consequently more or less prone to tolerate amino acid substitutions. In practical terms, the level of constraint can provide indications concerning which specific proteins or protein regions are better suited as possible targets for the development of antivirals or vaccines. Conversely, the current available knowledge and the analyses reported here allow no inference on the selective events (or lack thereof) that turned SARS-CoV-2 into a human pathogen. Recent analyses payed much attention to changes in the RBM. This is indeed expected to represent a major determinant of host range and its sequence is highly variable among SARS-CoV-related viruses (as also evident in Fig. 2). Albeit preliminary and necessarily limited to currently sampled genomes, our analyses suggest that recombination had a role in shaping the diversity of the RBMs in these viruses. Our data also indicate that divergence of SARS-CoV-2 from BatCoV RaTG13 was accompanied by limited episodes of positive selection, suggesting that the common ancestor of the two viruses was poised for human infection. We also emphasize that lack of knowledge about the reservoir host and the chain of events that determined the human spill-over prevent us from drawing any conclusion on the selective pressure underlying the limited positive selection events we detected. These will need to be interpreted in the future, by incorporating epidemiological, biochemical, and additional genetic data.

Clearly, a caveat of our analyses lies in the quality and paucity of SARS-CoV-2 genomes, as well as in the limited availability of genomes of other coronaviruses closely related to SARS-CoV-2. Available sequences were obtained using different methods and most likely contain errors. This is unlikely to strongly affect inference of positive selection, as the frequency of all selected sites is high in the SARS-CoV-2 population. Also, the SARS-CoV-2 sequences we analyzed display limited diversity (with only 41 nonsynonymous polymorphisms, most of them present in one or a few

sequences). Thus, although the availability of additional genomes may increase the power to detect selective events and the confidence with which evolutionary patterns are inferred, simply increasing the number of genomes is unlikely to change the bulk of our results. However, sustained viral spread in the human population will necessarily introduce new mutations in the viral population. Thus, data reported herein can only depict the situation of the early phases of the human epidemic. Follow-up analyses of the SARS-CoV-2 population will be required to determine the evolutionary trajectories of new mutations and to assess whether and how they affect viral fitness in the human hots.

Materials and Methods

Sequences and alignments

Genome sequences were retrieved from the National Center for Biotechnology Information database (NCBI, http://www.ncbi.nlm.nih.gov/). Only complete or almost complete genome sequences were included in the analysis (Table 1).

Alignments were generated using MAFFT (63), setting sequence type as codons.

Population genetics-phylogenetic analysis

Analyses were performed with gammaMap, that uses intra-species variation and inter-species diversity to estimate, along coding regions, the distribution of selection coefficients (γ). In this framework, γ is defined as $2PN_es$, where P is the ploidy, N_e is effective population size, and s is the fitness advantage of any amino acid-replacing derived allele (34).

For the eight longest ORFs in the SARS-CoV-2 genome, the corresponding coding sequence of BatCoV RaTG13 was used as the outgroup.

We assumed θ (neutral mutation rate per site), k (transitions/transversions ratio), and T (branch length) to vary within genes following log-normal distributions, whereas p (probability of adjacent codons to share the same selection coefficient) following a log-uniform distribution. For each ORF we set the neutral frequencies of non-STOP codons (1/61). For selection coefficients, we considered a uniform Dirichlet distribution with the same prior weight for each selection class. For each ORF we performed 2 runs with 100,000 iterations each and with a thinning interval of 10 iterations. Runs were merged after checking for convergence.

The similarity plot was computed using a Kimura (two-parameter) distance model with SimPlot version 3.5.1 (64). The strip gap option was set at the 50% default value. Similarity scores were calculated in sliding windows of 250 bp moving with a step of 50 bp.

Protein 3D structures and homology modeling

The structures of SARS-CoV N (PDB ID:2CJR) (65) and S (PDB ID: 6ACG)(48) proteins were obtained from the Protein Data Bank (PDB).

Homology modeling analysis was performed through the SWISS-MODEL server (66). The accuracy of the models was examined through the GMQE (Global Model Quality Estimation) and QMEAN (Qualitative Model Energy ANalysis) scores (67).

3D structures were rendered using PyMOL (The PyMOL Molecular Graphics System, Version 1.8.4.0 Schrödinger, LLC).

Acknowledgments

This work was supported by the Italian Ministry of Health ("Ricerca Corrente 2019-2020" to MS, "Ricerca Corrente 2018-2020" to DF)

References

1. **Coronaviridae Study Group of the International Committee on Taxonomy,of Viruses.** 2020. The species *Severe acute respiratory syndrome-related coronavirus*: classifying 2019-nCoV and naming it SARS-CoV-2. Nature Microbiology. **5**:536-544. doi: 10.1038/s41564-020-0695-z.

2. **Zhu, N., D. Zhang, W. Wang, X. Li, B. Yang, J. Song, X. Zhao, B. Huang, W. Shi, R. Lu, P. Niu, F. Zhan, X. Ma, D. Wang, W. Xu, G. Wu, G. F. Gao, W. Tan, and China Novel Coronavirus Investigating and Research Team.** 2020. A Novel Coronavirus from Patients with Pneumonia in China, 2019. N. Engl. J. Med. **382**:727-733. doi: 10.1056/NEJMoa2001017.

3. **Cui, J., F. Li, and Z. L. Shi.** 2019. Origin and evolution of pathogenic coronaviruses. Nat. Rev. Microbiol. **17:**181-192. doi: 10.1038/s41579-018-0118-9.

4. **Forni, D., R. Cagliani, M. Clerici, and M. Sironi.** 2017. Molecular Evolution of Human Coronavirus Genomes. Trends Microbiol. **25:**35-48. doi: S0966-842X(16)30133-0.

5. **Luk, H. K. H., X. Li, J. Fung, S. K. P. Lau, and P. C. Y. Woo.** 2019. Molecular epidemiology, evolution and phylogeny of SARS coronavirus. Infect. Genet. Evol. **71:**21-30. doi: S1567-1348(19)30031-0.

6. **de Groot, R. J., S. C. Baker, R. S. Baric, C. S. Brown, C. Drosten, L. Enjuanes, R. A. Fouchier, M. Galiano, A. E. Gorbalenya, Z. A. Memish, S. Perlman, L. L. Poon, E. J. Snijder, G. M. Stephens, P. C. Woo, A. M. Zaki, M. Zambon, and J. Ziebuhr.** 2013. Middle East respiratory syndrome coronavirus (MERS-CoV): announcement of the Coronavirus Study Group. J. Virol. **87:**7790-7792. doi: 10.1128/JVI.01244-13.

7. **Gorbalenya, A. E., E. J. Snijder, and W. J. Spaan.** 2004. Severe acute respiratory syndrome coronavirus phylogeny: toward consensus. J. Virol. **78:**7863-7866. doi: 10.1128/JVI.78.15.7863-7866.2004.

8. **Zhou, P., X. L. Yang, X. G. Wang, B. Hu, L. Zhang, W. Zhang, H. R. Si, Y. Zhu, B. Li, C. L. Huang, H. D. Chen, J. Chen, Y. Luo, H. Guo, R. D. Jiang, M. Q. Liu, Y. Chen, X. R. Shen, X. Wang, X. S. Zheng, K. Zhao, Q. J. Chen, F. Deng, L. L. Liu, B. Yan, F. X. Zhan, Y. Y. Wang, G. F. Xiao, and Z. L. Shi.** 2020. A pneumonia outbreak associated with a new coronavirus of probable bat origin. Nature. **579**:270-273. doi: 10.1038/s41586-020-2012-7.

9. **Wu, F., S. Zhao, B. Yu, Y. M. Chen, W. Wang, Z. G. Song, Y. Hu, Z. W. Tao, J. H. Tian, Y. Y. Pei, M. L. Yuan, Y. L. Zhang, F. H. Dai, Y. Liu, Q. M. Wang, J. J. Zheng, L. Xu, E. C. Holmes, and Y. Z. Zhang.** 2020. A new coronavirus associated with human respiratory disease in China. Nature. **579**:265-269. doi: 10.1038/s41586-020-2008-3.

10. **Hu, B., L. P. Zeng, X. L. Yang, X. Y. Ge, W. Zhang, B. Li, J. Z. Xie, X. R. Shen, Y. Z. Zhang, N. Wang, D. S. Luo, X. S. Zheng, M. N. Wang, P. Daszak, L. F. Wang, J. Cui, and Z. L. Shi.** 2017. Discovery of a rich gene pool of bat SARS-related coronaviruses provides new insights into the origin of SARS coronavirus. PLoS Pathog. **13:**e1006698. doi: 10.1371/journal.ppat.1006698.

11. **Wang, L., S. Fu, Y. Cao, H. Zhang, Y. Feng, W. Yang, K. Nie, X. Ma, and G. Liang.** 2017. Discovery and genetic analysis of novel coronaviruses in least horseshoe bats in southwestern China. Emerg. Microbes Infect. **6:**e14. doi: 10.1038/emi.2016.140.

12. **Lu, R., X. Zhao, J. Li, P. Niu, B. Yang, H. Wu, W. Wang, H. Song, B. Huang, N. Zhu, Y. Bi, X. Ma, F. Zhan, L. Wang, T. Hu, H. Zhou, Z. Hu, W. Zhou, L. Zhao, J. Chen, Y. Meng, J. Wang, Y. Lin, J. Yuan, Z. Xie, J. Ma, W. J. Liu, D. Wang, W. Xu, E. C. Holmes, G. F. Gao, G. Wu, W. Chen, W. Shi, and W. Tan.** 2020. Genomic characterization and epidemiology of 2019

358 novel coronavirus: implications for virus origins and receptor binding. Lancet. **395**:565-574. doi:
359 S0140-6736(20)30251-8.
360 13. **Paraskevis, D., E. G. Kostaki, G. Magiorkinis, G. Panayiotakopoulos, G. Sourvinos, and S.**
361 **Tsiodras.** 2020. Full-genome evolutionary analysis of the novel corona virus (2019-nCoV) rejects
362 the hypothesis of emergence as a result of a recent recombination event. Infect. Genet. Evol.
363 **79:**104212. doi: S1567-1348(20)30044-7.
364 14. **Lam, T. T., M. H. Shum, H. Zhu, Y. Tong, X. Ni, Y. Liao, W. Wei, W. Y. Cheung, W. Li, L.**
365 **Li, G. M. Leung, E. C. Holmes, Y. Hu, and Y. Guan.** 2020. Identification of 2019-nCoV related
366 coronaviruses in Malayan pangolins in southern China. Biorxiv. 2020.02.13.945485. doi:
367 10.1101/2020.02.13.945485.
368 15. **Xiao, K., J. Zhai, Y. Feng, N. Zhou, X. Zhang, J. Zou, N. Li, Y. Guo, X. Li, X. Shen, Z.**
369 **Zhang, F. Shu, W. Huang, Y. Li, Z. Zhang, R. Chen, Y. Wu, S. Peng, M. Huang, W. Xie, Q.**
370 **Cai, F. Hou, Y. Liu, W. Chen, L. Xiao, and Y. Shen.** 2020. Isolation and Characterization of 2019-
371 nCoV-like Coronavirus from Malayan Pangolins. Biorxiv. 2020.02.17.951335. doi:
372 10.1101/2020.02.17.951335.
373 16. **Wong, M. C., S. J. Javornik Cregeen, N. J. Ajami, and J. F. Petrosino.** 2020. Evidence of
374 recombination in coronaviruses implicating pangolin origins of nCoV-2019. Biorxiv.
375 2020.02.07.939207. doi: 10.1101/2020.02.07.939207.
376 17. **Liu, P., J. Jiang, X. Wan, Y. Hua, X. Wang, F. Hou, J. Chen, J. Zou, and J. Chen.** 2020. Are
377 pangolins the intermediate host of the 2019 novel coronavirus (2019-nCoV) ? Biorxiv.
378 2020.02.18.954628. doi: 10.1101/2020.02.18.954628.
379 18. **Haijema, B. J., H. Volders, and P. J. Rottier.** 2003. Switching species tropism: an effective
380 way to manipulate the feline coronavirus genome. J. Virol. **77:**4528-4538. doi:
381 10.1128/jvi.77.8.4528-4538.2003.

19. **Kuo, L., G. J. Godeke, M. J. Raamsman, P. S. Masters, and P. J. Rottier.** 2000. Retargeting of coronavirus by substitution of the spike glycoprotein ectodomain: crossing the host cell species barrier. J. Virol. **74:**1393-1406. doi: 10.1128/jvi.74.3.1393-1406.2000.

20. **McCray, P. B.,Jr, L. Pewe, C. Wohlford-Lenane, M. Hickey, L. Manzel, L. Shi, J. Netland, H. P. Jia, C. Halabi, C. D. Sigmund, D. K. Meyerholz, P. Kirby, D. C. Look, and S. Perlman.** 2007. Lethal infection of K18-hACE2 mice infected with severe acute respiratory syndrome coronavirus. J. Virol. **81:**813-821. doi: JVI.02012-06.

21. **Moore, M. J., T. Dorfman, W. Li, S. K. Wong, Y. Li, J. H. Kuhn, J. Coderre, N. Vasilieva, Z. Han, T. C. Greenough, M. Farzan, and H. Choe.** 2004. Retroviruses pseudotyped with the severe acute respiratory syndrome coronavirus spike protein efficiently infect cells expressing angiotensin-converting enzyme 2. J. Virol. **78:**10628-10635. doi: 10.1128/JVI.78.19.10628-10635.2004.

22. **Schickli, J. H., L. B. Thackray, S. G. Sawicki, and K. V. Holmes.** 2004. The N-terminal region of the murine coronavirus spike glycoprotein is associated with the extended host range of viruses from persistently infected murine cells. J. Virol. **78:**9073-9083. doi: 10.1128/JVI.78.17.9073-9083.2004.

23. **Li, W., M. J. Moore, N. Vasilieva, J. Sui, S. K. Wong, M. A. Berne, M. Somasundaran, J. L. Sullivan, K. Luzuriaga, T. C. Greenough, H. Choe, and M. Farzan.** 2003. Angiotensin-converting enzyme 2 is a functional receptor for the SARS coronavirus. Nature. **426:**450-454. doi: 10.1038/nature02145.

24. **Li, W., C. Zhang, J. Sui, J. H. Kuhn, M. J. Moore, S. Luo, S. K. Wong, I. C. Huang, K. Xu, N. Vasilieva, A. Murakami, Y. He, W. A. Marasco, Y. Guan, H. Choe, and M. Farzan.** 2005. Receptor and viral determinants of SARS-coronavirus adaptation to human ACE2. Embo J. **24:**1634-1643. doi: 7600640.

406 25. **Wu, K., G. Peng, M. Wilken, R. J. Geraghty, and F. Li.** 2012. Mechanisms of host receptor
407 adaptation by severe acute respiratory syndrome coronavirus. J. Biol. Chem. **287:**8904-8911. doi:
408 10.1074/jbc.M111.325803.
409 26. **Qu, X. X., P. Hao, X. J. Song, S. M. Jiang, Y. X. Liu, P. G. Wang, X. Rao, H. D. Song, S. Y.**
410 **Wang, Y. Zuo, A. H. Zheng, M. Luo, H. L. Wang, F. Deng, H. Z. Wang, Z. H. Hu, M. X. Ding,**
411 **G. P. Zhao, and H. K. Deng.** 2005. Identification of two critical amino acid residues of the severe
412 acute respiratory syndrome coronavirus spike protein for its variation in zoonotic tropism transition
413 via a double substitution strategy. J. Biol. Chem. **280:**29588-29595. doi: M500662200.
414 27. **Chinese SARS Molecular Epidemiology Consortium.** 2004. Molecular evolution of the
415 SARS coronavirus during the course of the SARS epidemic in China. Science. **303:**1666-1669. doi:
416 10.1126/science.1092002.
417 28. **Lau, S. K., Y. Feng, H. Chen, H. K. Luk, W. H. Yang, K. S. Li, Y. Z. Zhang, Y. Huang, Z. Z.**
418 **Song, W. N. Chow, R. Y. Fan, S. S. Ahmed, H. C. Yeung, C. S. Lam, J. P. Cai, S. S. Wong, J. F.**
419 **Chan, K. Y. Yuen, H. L. Zhang, and P. C. Woo.** 2015. Severe Acute Respiratory Syndrome
420 (SARS) Coronavirus ORF8 Protein Is Acquired from SARS-Related Coronavirus from Greater
421 Horseshoe Bats through Recombination. J. Virol. **89:**10532-10547. doi: 10.1128/JVI.01048-15.
422 29. **Muth, D., V. M. Corman, H. Roth, T. Binger, R. Dijkman, L. T. Gottula, F. Gloza-Rausch,**
423 **A. Balboni, M. Battilani, D. Rihtaric, I. Toplak, R. S. Ameneiros, A. Pfeifer, V. Thiel, J. F.**
424 **Drexler, M. A. Muller, and C. Drosten.** 2018. Attenuation of replication by a 29 nucleotide
425 deletion in SARS-coronavirus acquired during the early stages of human-to-human transmission.
426 Sci. Rep. **8:**15177. doi: 10.1038/s41598-018-33487-8.
427 30. **Chan, J. F., S. Yuan, K. H. Kok, K. K. To, H. Chu, J. Yang, F. Xing, J. Liu, C. C. Yip, R. W.**
428 **Poon, H. W. Tsoi, S. K. Lo, K. H. Chan, V. K. Poon, W. M. Chan, J. D. Ip, J. P. Cai, V. C.**
429 **Cheng, H. Chen, C. K. Hui, and K. Y. Yuen.** 2020. A familial cluster of pneumonia associated

with the 2019 novel coronavirus indicating person-to-person transmission: a study of a family cluster. Lancet. **395**:514-523. doi: S0140-6736(20)30154-9.

31. **Li, Q., X. Guan, P. Wu, X. Wang, L. Zhou, Y. Tong, R. Ren, K. S. M. Leung, E. H. Y. Lau, J. Y. Wong, X. Xing, N. Xiang, Y. Wu, C. Li, Q. Chen, D. Li, T. Liu, J. Zhao, M. Li, W. Tu, C. Chen, L. Jin, R. Yang, Q. Wang, S. Zhou, R. Wang, H. Liu, Y. Luo, Y. Liu, G. Shao, H. Li, Z. Tao, Y. Yang, Z. Deng, B. Liu, Z. Ma, Y. Zhang, G. Shi, T. T. Y. Lam, J. T. K. Wu, G. F. Gao, B. J. Cowling, B. Yang, G. M. Leung, and Z. Feng.** 2020. Early Transmission Dynamics in Wuhan, China, of Novel Coronavirus-Infected Pneumonia. In press. N. Engl. J. Med. . doi: 10.1056/NEJMoa2001316.

32. **Phan, L. T., T. V. Nguyen, Q. C. Luong, T. V. Nguyen, H. T. Nguyen, H. Q. Le, T. T. Nguyen, T. M. Cao, and Q. D. Pham.** 2020. Importation and Human-to-Human Transmission of a Novel Coronavirus in Vietnam. N. Engl. J. Med. **382:**872-874. doi: 10.1056/NEJMc2001272.

33. **Chinazzi, M., J. T. Davis, M. Ajelli, C. Gioannini, M. Litvinova, S. Merler, A. Pastore Y Piontti, K. Mu, L. Rossi, K. Sun, C. Viboud, X. Xiong, H. Yu, M. E. Halloran, I. M. Longini Jr, and A. Vespignani.** 2020. The effect of travel restrictions on the spread of the 2019 novel coronavirus (COVID-19) outbreak. Science. In press. doi: eaba9757.

34. **Wilson, D. J., R. D. Hernandez, P. Andolfatto, and M. Przeworski.** 2011. A population genetics-phylogenetics approach to inferring natural selection in coding sequences. PLoS Genet. **7:**e1002395. doi: 10.1371/journal.pgen.1002395.

35. **Ho, S. Y., R. Lanfear, L. Bromham, M. J. Phillips, J. Soubrier, A. G. Rodrigo, and A. Cooper.** 2011. Time-dependent rates of molecular evolution. Mol. Ecol. **20:**3087-3101. doi: 10.1111/j.1365-294X.2011.05178.x.

36. **Wertheim, J. O., and S. L. Kosakovsky Pond.** 2011. Purifying selection can obscure the ancient age of viral lineages. Mol. Biol. Evol. **28:**3355-3365. doi: 10.1093/molbev/msr170.

454 37. **Wertheim, J. O., D. K. Chu, J. S. Peiris, S. L. Kosakovsky Pond, and L. L. Poon.** 2013. A
455 case for the ancient origin of coronaviruses. J. Virol. **87:**7039-7045. doi: 10.1128/JVI.03273-12.
456 38. **Snijder, E. J., E. Decroly, and J. Ziebuhr.** 2016. The Nonstructural Proteins Directing
457 Coronavirus RNA Synthesis and Processing. Adv. Virus Res. **96:**59-126. doi: S0065-
458 3527(16)30047-1.
459 39. **Armstrong, J., H. Niemann, S. Smeekens, P. Rottier, and G. Warren.** 1984. Sequence and
460 topology of a model intracellular membrane protein, E1 glycoprotein, from a coronavirus. Nature.
461 **308:**751-752. doi: 10.1038/308751a0.
462 40. **Siu, Y. L., K. T. Teoh, J. Lo, C. M. Chan, F. Kien, N. Escriou, S. W. Tsao, J. M. Nicholls, R.**
463 **Altmeyer, J. S. M. Peiris, R. Bruzzone, and B. Nal.** 2008. The M, E, and N structural proteins of
464 the severe acute respiratory syndrome coronavirus are required for efficient assembly, trafficking,
465 and release of virus-like particles. J. Virol. **82:**11318-11330. doi: 10.1128/JVI.01052-08.
466 41. **Liu, J., Y. Sun, J. Qi, F. Chu, H. Wu, F. Gao, T. Li, J. Yan, and G. F. Gao.** 2010. The
467 membrane protein of severe acute respiratory syndrome coronavirus acts as a dominant immunogen
468 revealed by a clustering region of novel functionally and structurally defined cytotoxic T-
469 lymphocyte epitopes. J. Infect. Dis. **202:**1171-1180. doi: 10.1086/656315.
470 42. **Pang, H., Y. Liu, X. Han, Y. Xu, F. Jiang, D. Wu, X. Kong, M. Bartlam, and Z. Rao.** 2004.
471 Protective humoral responses to severe acute respiratory syndrome-associated coronavirus:
472 implications for the design of an effective protein-based vaccine. J. Gen. Virol. **85:**3109-3113. doi:
473 10.1099/vir.0.80111-0.
474 43. **Narayanan, K., S. I. Ramirez, K. G. Lokugamage, and S. Makino.** 2015. Coronavirus
475 nonstructural protein 1: Common and distinct functions in the regulation of host and viral gene
476 expression. Virus Res. **202:**89-100. doi: 10.1016/j.virusres.2014.11.019.

44. **Neuman, B. W.** 2016. Bioinformatics and functional analyses of coronavirus nonstructural proteins involved in the formation of replicative organelles. Antiviral Res. **135:**97-107. doi: 10.1016/j.antiviral.2016.10.005.

45. **Brand, C. L., M. V. Cattani, S. B. Kingan, E. L. Landeen, and D. C. Presgraves.** 2018. Molecular Evolution at a Meiosis Gene Mediates Species Differences in the Rate and Patterning of Recombination. Curr. Biol. **28:**1289-1295.e4. doi: S0960-9822(18)30241-0.

46. **Hemmer, L. W., and J. P. Blumenstiel.** 2016. Holding it together: rapid evolution and positive selection in the synaptonemal complex of Drosophila. BMC Evol. Biol. **16:**91. doi: 10.1186/s12862-016-0670-8.

47. **Li, F., W. Li, M. Farzan, and S. C. Harrison.** 2005. Structure of SARS coronavirus spike receptor-binding domain complexed with receptor. Science. **309:**1864-1868. doi: 309/5742/1864.

48. **Song, W., M. Gui, X. Wang, and Y. Xiang.** 2018. Cryo-EM structure of the SARS coronavirus spike glycoprotein in complex with its host cell receptor ACE2. PLoS Pathog. **14:**e1007236. doi: 10.1371/journal.ppat.1007236.

49. **Graham, R. L., and R. S. Baric.** 2010. Recombination, reservoirs, and the modular spike: mechanisms of coronavirus cross-species transmission. J. Virol. **84:**3134-3146. doi: 10.1128/JVI.01394-09.

50. **Martin, D. P., B. Murrell, A. Khoosal, and B. Muhire.** 2017. Detecting and Analyzing Genetic Recombination Using RDP4. Methods Mol. Biol. **1525:**433-460. doi: 10.1007/978-1-4939-6622-6_17.

51. **Martin, D. P., P. Lemey, and D. Posada.** 2011. Analysing recombination in nucleotide sequences. Mol. Ecol. Resour. **11:**943-955. doi: 10.1111/j.1755-0998.2011.03026.x.

52. **Takeda, M., C. K. Chang, T. Ikeya, P. Guntert, Y. H. Chang, Y. L. Hsu, T. H. Huang, and M. Kainosho.** 2008. Solution structure of the c-terminal dimerization domain of SARS coronavirus

nucleocapsid protein solved by the SAIL-NMR method. J. Mol. Biol. **380:**608-622. doi: 10.1016/j.jmb.2007.11.093.

53. **Chang, C. K., M. H. Hou, C. F. Chang, C. D. Hsiao, and T. H. Huang.** 2014. The SARS coronavirus nucleocapsid protein--forms and functions. Antiviral Res. **103:**39-50. doi: 10.1016/j.antiviral.2013.12.009.

54. **Surjit, M., and S. K. Lal.** 2008. The SARS-CoV nucleocapsid protein: a protein with multifarious activities. Infect. Genet. Evol. **8:**397-405. doi: S1567-1348(07)00102-5.

55. **Wathelet, M. G., M. Orr, M. B. Frieman, and R. S. Baric.** 2007. Severe acute respiratory syndrome coronavirus evades antiviral signaling: role of nsp1 and rational design of an attenuated strain. J. Virol. **81:**11620-11633. doi: JVI.00702-07.

56. **Brockway, S. M., and M. R. Denison.** 2005. Mutagenesis of the murine hepatitis virus nsp1-coding region identifies residues important for protein processing, viral RNA synthesis, and viral replication. Virology. **340:**209-223. doi: S0042-6822(05)00377-6.

57. **Zust, R., L. Cervantes-Barragan, T. Kuri, G. Blakqori, F. Weber, B. Ludewig, and V. Thiel.** 2007. Coronavirus non-structural protein 1 is a major pathogenicity factor: implications for the rational design of coronavirus vaccines. PLoS Pathog. **3:**e109. doi: 07-PLPA-RA-0063.

58. **Jauregui, A. R., D. Savalia, V. K. Lowry, C. M. Farrell, and M. G. Wathelet.** 2013. Identification of residues of SARS-CoV nsp1 that differentially affect inhibition of gene expression and antiviral signaling. PLoS One. **8:**e62416. doi: 10.1371/journal.pone.0062416.

59. **Pfefferle, S., J. Schopf, M. Kogl, C. C. Friedel, M. A. Muller, J. Carbajo-Lozoya, T. Stellberger, E. von Dall'Armi, P. Herzog, S. Kallies, D. Niemeyer, V. Ditt, T. Kuri, R. Zust, K. Pumpor, R. Hilgenfeld, F. Schwarz, R. Zimmer, I. Steffen, F. Weber, V. Thiel, G. Herrler, H. J. Thiel, C. Schwegmann-Wessels, S. Pohlmann, J. Haas, C. Drosten, and A. von Brunn.** 2011. The SARS-coronavirus-host interactome: identification of cyclophilins as target for pan-coronavirus inhibitors. PLoS Pathog. **7:**e1002331. doi: 10.1371/journal.ppat.1002331.

60. **Jimenez-Guardeno, J. M., J. A. Regla-Nava, J. L. Nieto-Torres, M. L. DeDiego, C. Castano-Rodriguez, R. Fernandez-Delgado, S. Perlman, and L. Enjuanes.** 2015. Identification of the Mechanisms Causing Reversion to Virulence in an Attenuated SARS-CoV for the Design of a Genetically Stable Vaccine. PLoS Pathog. **11:**e1005215. doi: 10.1371/journal.ppat.1005215.

61. **Oostra, M., C. A. de Haan, and P. J. Rottier.** 2007. The 29-nucleotide deletion present in human but not in animal severe acute respiratory syndrome coronaviruses disrupts the functional expression of open reading frame 8. J. Virol. **81:**13876-13888. doi: JVI.01631-07.

62. **Sung, S. C., C. Y. Chao, K. S. Jeng, J. Y. Yang, and M. M. Lai.** 2009. The 8ab protein of SARS-CoV is a luminal ER membrane-associated protein and induces the activation of ATF6. Virology. **387:**402-413. doi: 10.1016/j.virol.2009.02.021.

63. **Katoh, K., and D. M. Standley.** 2013. MAFFT multiple sequence alignment software version 7: improvements in performance and usability. Mol. Biol. Evol. **30:**772-780. doi: 10.1093/molbev/mst010; 10.1093/molbev/mst010.

64. **Lole, K. S., R. C. Bollinger, R. S. Paranjape, D. Gadkari, S. S. Kulkarni, N. G. Novak, R. Ingersoll, H. W. Sheppard, and S. C. Ray.** 1999. Full-length human immunodeficiency virus type 1 genomes from subtype C-infected seroconverters in India, with evidence of intersubtype recombination. J. Virol. **73:**152-160.

65. **Chen, C., C. Chang, Y. Chang, S. Sue, H. Bai, L. Riang, C. Hsiao, and T. Huang.** 2007. Structure of the SARS coronavirus nucleocapsid protein RNA-binding dimerization domain suggests a mechanism for helical packaging of viral RNA. J. Mol. Biol. **368:**1075-1086. doi: 10.1016/j.jmb.2007.02.069.

66. **Biasini, M., S. Bienert, A. Waterhouse, K. Arnold, G. Studer, T. Schmidt, F. Kiefer, T. Gallo Cassarino, M. Bertoni, L. Bordoli, and T. Schwede.** 2014. SWISS-MODEL: modelling protein tertiary and quaternary structure using evolutionary information. Nucleic Acids Res. **42:**W252-8. doi: 10.1093/nar/gku340.

551 67. **Benkert, P., M. Biasini, and T. Schwede.** 2011. Toward the estimation of the absolute quality
552 of individual protein structure models. Bioinformatics. **27:**343-350. doi:
553 10.1093/bioinformatics/btq662.
554 68. **Lei, J., Y. Kusov, and R. Hilgenfeld.** 2018. Nsp3 of coronaviruses: Structures and functions of
555 a large multi-domain protein. Antiviral Res. **149**:58-74. doi: 10.1016/j.antiviral.2017.11.001.
556 69. **Chan, J. F., K. H. Kok, Z. Zhu, H. Chu, K. K. To, S. Yuan, and K. Y. Yuen.** 2020. Genomic
557 characterization of the 2019 novel human-pathogenic coronavirus isolated from a patient with
558 atypical pneumonia after visiting Wuhan. Emerg. Microbes Infect. **9:**221-236. doi:
559 10.1080/22221751.2020.1719902.
560 70. **Coutard, B., C. Valle, X. de Lamballerie, B. Canard, N. G. Seidah, and E. Decroly.** 2020.
561 The spike glycoprotein of the new coronavirus 2019-nCoV contains a furin-like cleavage site absent
562 in CoV of the same clade. Antiviral Res. **176:**104742. doi: S0166-3542(20)30052-8.
563
564
565 **Figure legends**
566
567 **Figure 1. Selective patterns of SARS-CoV-2.** (A) Similarity plot (generated with SimPlot) of
568 BatCoV RaTG13 relative to SARS-CoV-2 (Wuhan-Hu-1 reference strain, NC_045512.2).
569 Similarity (Kimura distance) was calculated within sliding windows of 250 bp moving with a step
570 of 50 bp. A schematic representation of the SARS-CoV-2 genome is also shown. ORF and nsp (non-
571 structural protein) names, lengths, and relative positions are in accordance with the annotation for
572 the reference Wuhan-Hu-1 sequence. Box colors indicate the level of amino acid identity between
573 the SARS-CoV-2 and BatCoV RaTG13 sequences. Black triangles indicate amino acid changes that
574 are polymorphic in the analyzed SARS-CoV-2 genomes. Asterisks denote positively selected sites
575 and their size is proportional to the number of selected sites/region. Short ORFs with names in red

were not analyzed with gammaMap. Violin plots (median, white dot; interquartile range, black bar) of selection coefficients (γ) for the longest (more that 80 codons) ORFs (B) and nsp3 sub-domains (C) are shown. Nsp3 domains were retrieved from the SARS-CoV annotation (68).

Figure 2. SARS-CoV-2 positively selected sites. Schematic representation of the nsp1, ORF8, Spike (S), and nucleocapsid (N) proteins. Positively selected sites (magenta), amino acid substitutions between SARS-CoV-2 and BatCoV RaTG13 (red), and between SARS-CoV-2 and pangolin-CoV MP789 (blue) are reported in the alignments.
The location of an insertion (insPRRA) in the spike glycoprotein is also shown. This insertion is predicted to occur in the S1/S2 furin-like cleavage site (69, 70).

Figure 3. Homology modeling of positively selected SARS-CoV-2 proteins. Selected sites are mapped onto the 3D structure of models obtained using SARS-CoV proteins as a templates (PDB ID: 6ACG for panel A, 2CJR for panel B, 2HSX for panel C). Coronavirus proteins are colored in hues of blue based on the most likely selection coefficient. Positively selected sites are marked in red. (A) Ribbon representation of the spike glycoprotein model (one monomer is shown) in complex with human ACE2 (green) (48). The binding interface is shown in the enlargement. (B) Ribbon representation of the C-terminal domain of the nucleocapsid protein. (C) Ribbon representation of the N-terminal portion of nsp1. Note that although some sites had the highest posterior probability for $\gamma = 1$ (yellow), they were not called as positively selected because the 0.5 threshold was not reached.

Table 1. List of analyzed strains.

Strain Name	GenBank ID
Wuhan-Hu-1	NC_045512.2
2019-nCoV WHU01	MN988668.1
2019-nCoV WHU02	MN988669.1
2019-nCoV_HKU-SZ-005b_2020	MN975262.1
2019-nCoV_HKU-SZ-002a_2020	MN938384.1
SARS-CoV-2/WH-09/human/2020/CHN	MT093631.1
SARS-CoV-2/IQTC01/human/2020/CHN	MT123290.1
HZ-1	MT039873.1
BetaCoV/Wuhan/IPBCAMS-WH-01/2019	MT019529.1
BetaCoV/Wuhan/IPBCAMS-WH-03/2019	MT019531.1
BetaCoV/Wuhan/IPBCAMS-WH-02/2019	MT019530.1
BetaCoV/Wuhan/IPBCAMS-WH-04/2019	MT019532.1
BetaCoV/Wuhan/IPBCAMS-WH-05/2020	MT019533.1
WIV02	MN996527.1
WIV04	MN996528.1
WIV05	MN996529.1
WIV06	MN996530.1
WIV07	MN996531.1
SARS-CoV-2/Yunnan-01/human/2020/CHN	MT049951.1
nCoV-FIN-29-Jan-2020	MT020781.1
SARS0CoV-2/61-TW/human/2020/ NPL	MT072688.1
SNU01	MT039890.1
SARS-CoV-2/01/human/2020/SWE	MT093571.1
SARS-CoV-2/NTU01/2020/TWN	MT066175.1
SARS-CoV-2/NTU02/2020/TWN	MT066176.1
2019-nCoV/USA-WA1/2020	MN985325.1
2019-nCoV/USA-AZ1/2020	MN997409.1
2019-nCoV/USA-CA1/2020	MN994467.1
2019-nCoV/USA-CA2/2020	MN994468.1
2019-nCoV/USA-CA3/2020	MT027062.1
2019-nCoV/USA-CA4/2020	MT027063.1
2019-nCoV/USA-CA5/2020	MT027064.1
2019-nCoV/USA-CA6/2020	MT044258.1
2019-nCoV/USA-CA7/2020	MT106052.1

2019-nCoV/USA-CA8/2020	MT106053.1
2019-nCoV/USA-CA9/2020	MT118835.1
2019-nCoV/USA-IL2/2020	MT044257.1
2019-nCoV/USA-IL1/2020	MN988713.1
2019-nCoV/USA-MA1/2020	MT039888.1
2019-nCoV/USA-TX1/2020	MT106054.1
2019-nCoV/USA-WA1-A12/2020	MT020880.1
2019-nCoV/USA-WA1-F6/2020	MT020881.1
2019-nCoV/USA-WI1/2020	MT039887.1
Australia/VIC01/2020	MT007544.1
Bat coronavirus RaTG13	MN996532.1
Pangolin coronavirus isolate MP789	MT084071.1
Bat SARS-like coronavirus isolate bat-SL-CoVZC45	MG772933.1
Bat SARS-like coronavirus isolate bat-SL-CoVZXC21	MG772934.1
SARS-CoV tor2	NC_004718.3
SARS-CoV GZ02	AY390556.1
Bat SARS coronavirus HKU3-1	DQ022305.2
Rhinolophus affinis coronavirus isolate LYRa11	KF569996.1

602
603

604

A

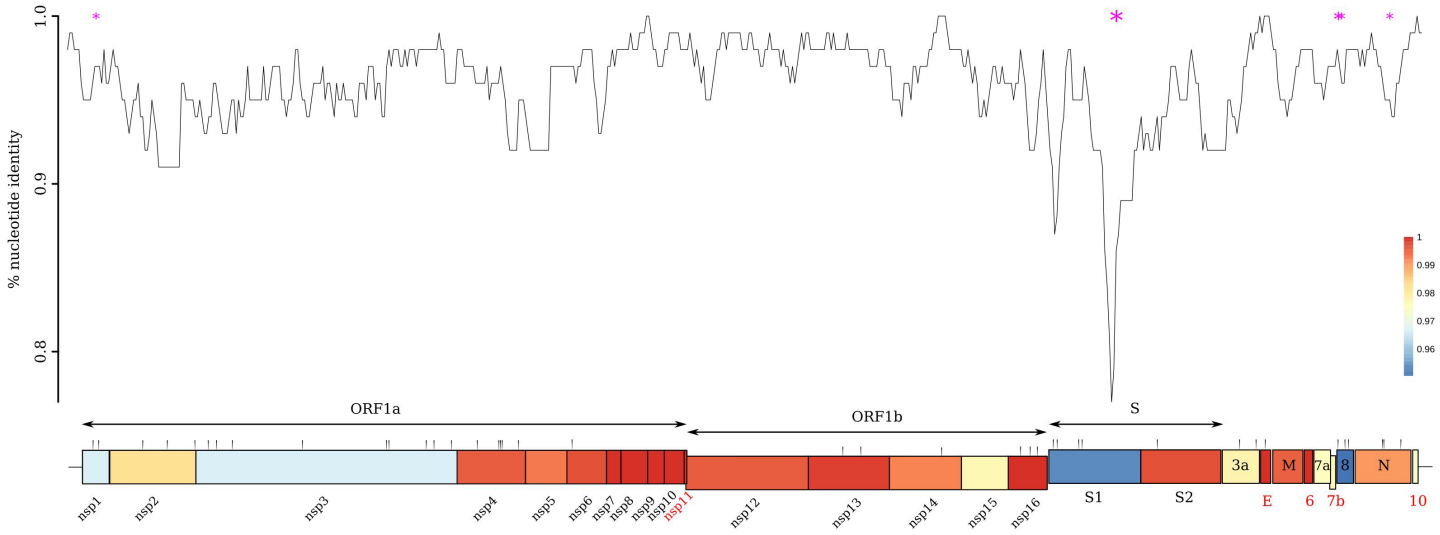
% nucleotide identity
1.0
0.9
0.8
ORF1a
ORF1b
S
nsp1
nsp2
nsp3
nsp4
nsp5
nsp6
nsp7
nsp8
nsp9
nsp10
nsp11
nsp12
nsp13
nsp14
nsp15
nsp16
S1
S2
3a
E
M
6
7a
7b
8
N
10

B

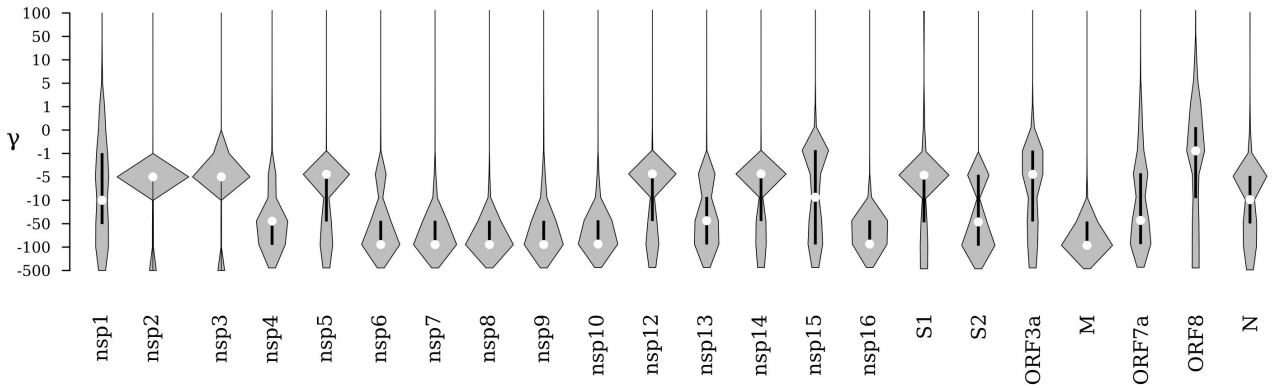
γ
100
50
10
5
1
0
-1
-5
-10
-50
-100
-500
nsp1
nsp2
nsp3
nsp4
nsp5
nsp6
nsp7
nsp8
nsp9
nsp10
nsp12
nsp13
nsp14
nsp15
nsp16
S1
S2
ORF3a
M
ORF7a
ORF8
N

C

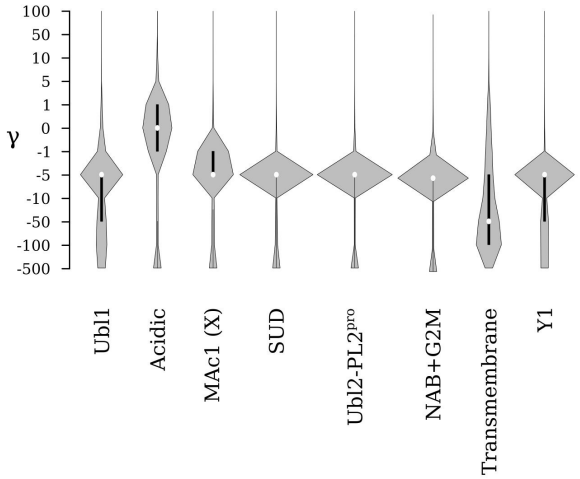
γ
100
50
10
5
1
0
-1
-5
-10
-50
-100
-500
Ubl1
Acidic
MAc1 (X)
SUD
Ubl2-PL2pro
NAB+G2M
Transmembrane
Y1

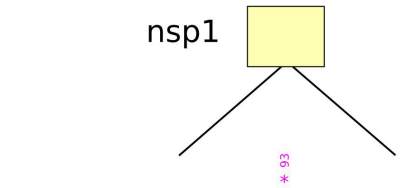


```
Wuhan-Hu-1          TAPHGHVMVELVAELEGIQYGRSGETLGVLV
BatCoV RaTG13       TAPHGHVMVELVAELNGIQYGRSGETLGVLV
Pangolin-CoV        TAPHGHVMVELVAELNGVQYGRSGETLGVLV
Bat-SL-CoVZC45      TAPHGHVMVELVAELDGIQYGRSGETLGVLV
Bat-SL-CoVZXC21     TAHHGHVMVELVAELDGIQYGRSGETLGVLV
Human-SARS-Tor2     STNHGHKVVELVAEMDGIQYGRSGITLGVLV
Bat-HKU3-1          STNHGHKVVELVAELDGIQFGRSGITLGVLV
Bat-lyra11          GTGHGHKVCELVAELDGVQFGRSGITLGVLV
```

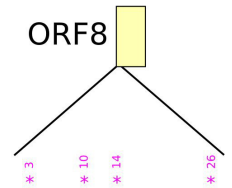


```
Wuhan-Hu-1          MKFLVFLGIITTVAAFHQECSLQSCTQH
BatCoV RaTG13       MKLLVFLGILTTVTAFHQECSLQSCAQH
Pangolin-CoV        MKFLVFLGILTTVTAFHQECSLQSCAQH
Bat-SL-CoVZC45      MKFLVFLGILTTVAAFHQECSLQSCAQH
Bat-SL-CoVZXC21     MKFLVFLGILTTVAAFHQECSLQSCAQH
Human-SARS-GZ02     MKLLIVLTCISLCSCIRT--VVQRCASN
Bat-HKU3-1          MKLLIVFGLLASVYCFHRECSIQECCEN
Bat-lyra11          MKLLIVFGLLTIVYGMHKECTIQECCEN
```

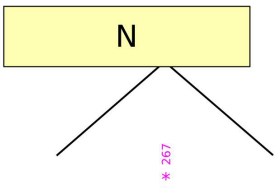


```
Wuhan-Hu-1          EASKKPRQKRTATKAYNVTQAFGRRGPEQ
BatCoV RaTG13       EASKKPRQKRTATKQYNVTQAFGRRGPEQ
Pangolin-CoV        EASKKPRQKRTATKQYNVTQAFGRRGPEQ
Bat-SL-CoVZC45      EASKKPRQKRTATKQYNVTQAFGRRGPEQ
Bat-SL-CoVZXC21     EASKKPRQKRTATKQYNVTQAFGRRGPEQ
Human-SARS-Tor2     EASKKPRQKRTATKQYNVTQAFGRRGPEQ
Bat-HKU3-1          EASKKPRQKRTATKQYNVTQAFGRRGPEQ
Bat-lyra11          EASKKPRQKRTATKAYNVTQAFGRRGPEQ
```

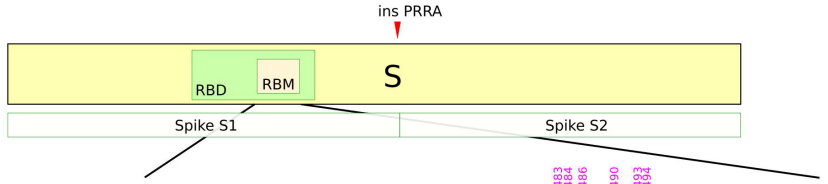


```
Wuhan-Hu-1          DDFTGCVIAWNSNNLDSKVGGNYNYLYRLFRKSNLKPFERDISTEIYQAGSTPCNGVEGFNCYFPLQSYGFQPTNGVGYQPYRVVVLSFELL
BatCoV RaTG13       DDFTGCVIAWNSKHIDAKEGGNFNYLYRLFRKANLKPFERDISTEIYQAGSKPCNGQTGLNCYYPLYRYGFYPTDGVGHQPYRVVVLSFELL
Pangolin-CoV        DDFTGCVIAWNSNNLDSKVGGNYNYLYRLFRKSNLKPFERDISTEIYQAGSTPCNGVEGFNCYFPLQSYGFHPTNGVGYQPYRVVVLSFELL
Bat-SL-CoVZC45      DDFTGCVIAWNTAKQDVG-----NYFYRSHRSTKLKPFERDLSSDE--------------NGVRTLSTYDFNPNVPLEYQATRVVVLSFELL
Bat-SL-CoVZXC21     DDFTGCVIAWNTAKQDTG-----HYFYRSHRSTKLKPFERDLSSDE--------------NGVRTLSTYDFNPNVPLEYQATRVVVLSFELL
Human-SARS-Tor2     DDFMGCVLAWNTRNIDATSTGNYNYKYRYLRHGKLRPFERDISNVPFSPDGKPCTP-PALNCYWPLNDYGFYTTTGIGYQPYRVVVLSFELL
Bat-HKU3-1          DDFTGCVIAWNTAKHDTG-----NYYYRSHRKTKLKPFERDLSSDDG-------------NGVYTLSTYDFNPNVPVAYQATRVVVLSFELL
Bat-lyra11          DDFMGCVLAWNTRNIDATSSGNFNYKYRSLRHGKLRPFERDISNVPFSPDGKPCTP-PAFNCYWPLNDYGFYTTNGIGYQPYRVVVLSFELL
```

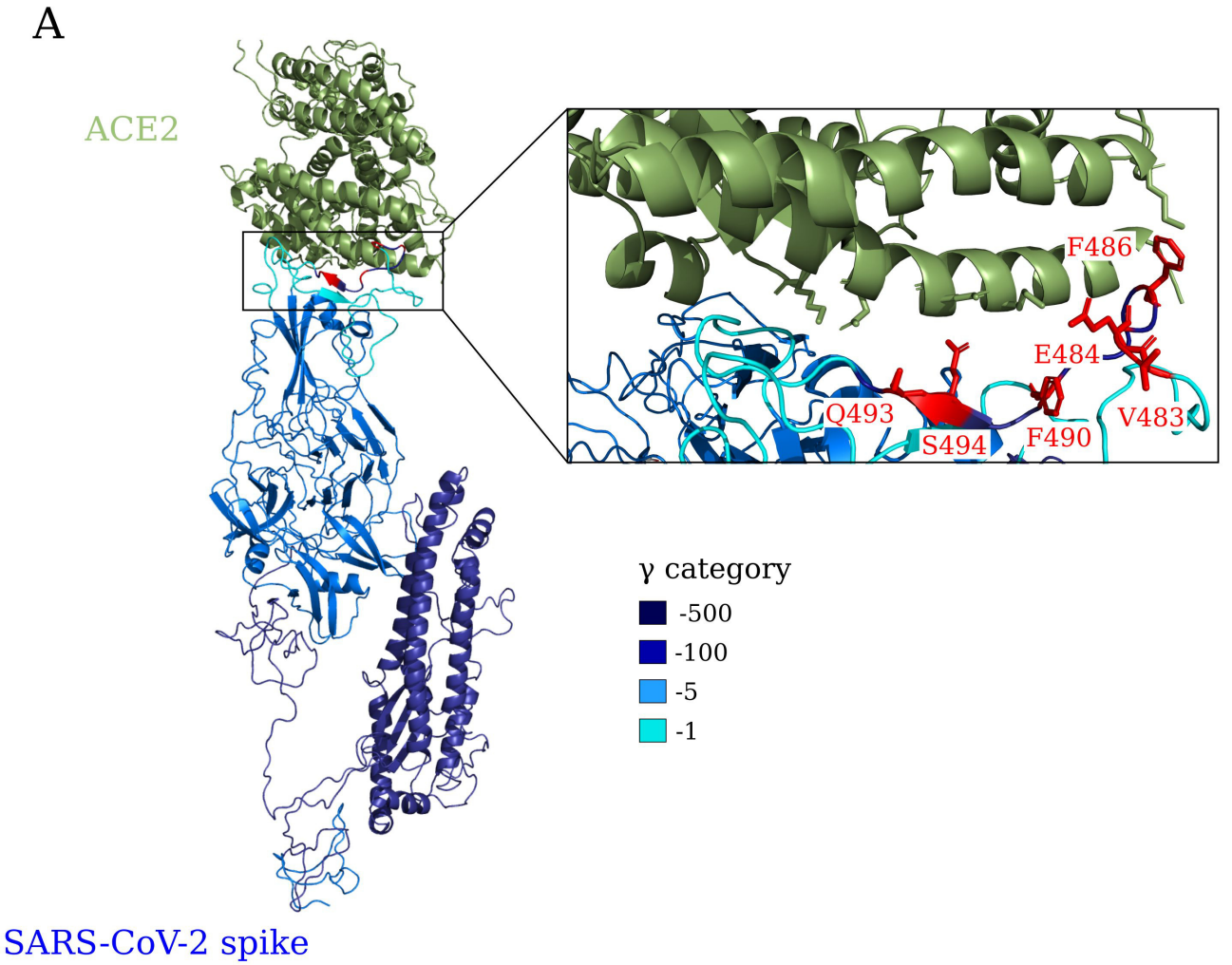
A
ACE2
F486
E484
Q493
S494
F490
V483
γ category
-500
-100
-5
-1
SARS-CoV-2 spike
B
A267
γ category
-50
-5
C
E93
γ category
-100
-5
-1
0
1